

# Research Journal of Pharmaceutical, Biological and Chemical Sciences

## Design, Synthesis, Characterization, DFT, and discovery potent based on DOCKING Studies for Novel amino acid derivatives as Anti-inflammatory Agent.

Ahmed A Elhenawy<sup>1\*</sup>, and MY Sameeh<sup>2</sup>.

<sup>1</sup>Chemistry Department, Faculty of Science, Al-Azhar University (Boys Branch), Nasr City, Cairo, Egypt.

<sup>2</sup>Chemistry Department, Faculty of Science, UmmAl-Qura University, Lieth, Saudi Arabia

### ABSTRACT

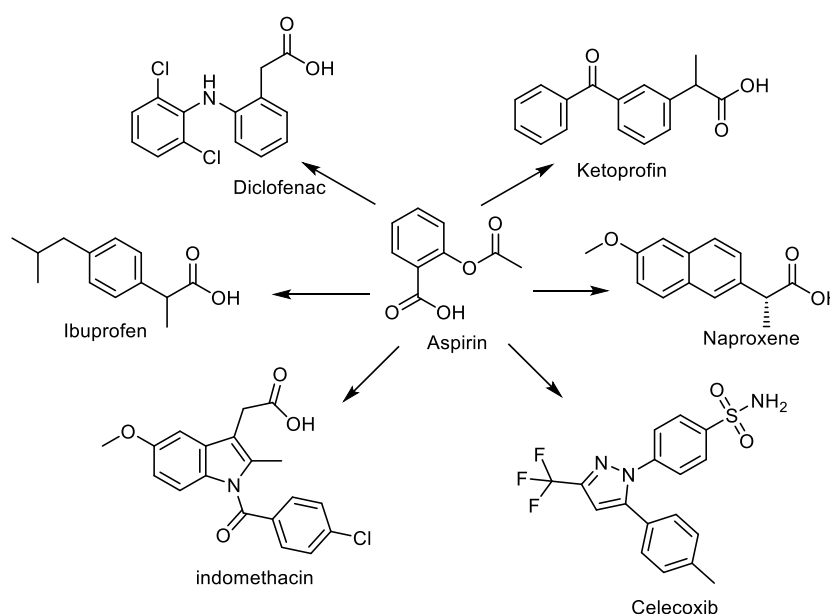
Several effective anticancer therapeutic drugs contain coumarin nucleus. This work aims to synthesize safe bioactive coumarin derivatives. The structures of these compounds 3, 4, 6-8, 10 and 11. Were established on the basis of spectral data. The optimization geometries, frontier molecular orbital's (FMOs), thermodynamic parameters, global chemical reactivities, were discussed using DFT\B3LYP with 6- 31G\* level of theory. The molecular electrostatic potentials (MEPs) were plotted for the elucidation interaction manner of synthesized compounds with the receptor, through investigation distribution negative and positive regions upon its compounds. The NLOs manner were elucidated via 1st and 2nd hyper polarize abilities. The molecular docking simulations into the active site of COX-2 were performed, and showed that, the compounds **3,5** and **6** are suitable inhibitor against COX-2, and can used as anti-cancer drugs. The ADMET profiles showed that, these compounds are good oral bioavailability.

**Keywords:** NASIDs; Anti- inflammatory; DFTADMET; DOCKIN.

*\*Corresponding author*

## INTRODUCTION

Non-steroidal anti-inflammatory drugs (NSAIDs) are widely employed, due to have anti-inflammatory properties [1], through inhibition of COX inhibitor (COX-1 and COX-2), over inhibiting the production of prostaglandins (PGs)[2, 3]. Due to non-selectively of NASIDs (Str. 1) inhibition of COX, and suffering from gastrointestinal as a common side effect [4-6]. Its drugs widely displayed anti-microbial properties[7-9], ulcerogenic, analgesic, anti-inflammatory[8], lipid peroxidation[9], antitumor [10], and inhibitor formation of transthyretin amyloid fibril properties[11]. Inundation, the alaninyl derivatives especially containing amide and thioamide moieties possesses diverse biological activities, such as anti-inflammatory, anti-tumor and antimicrobial activity [12-14]. Coumarin derivatives is a novel class of inhibitors of the carbonic anhydrase (CA)[15, 16], Hence, the present study aims to synthesis new series of NASIDs derivatives acting as new potent anti-inflammatory agents, without ulcerogenic effects, depending on molecular modeling to identify the structural features of these new series. The molecular docking was performed, to predict the correct binding geometry for each ligand at the active site, which may be support that postulation, the active compounds may be act as a new NASIDs.



Structure 1: Chemical structure of commonly used marking NASIDS

## MATERIALS AND METHODS

Melting points were taken on a Griffin melting point apparatus and are uncorrected. Thin layer chromatography (RF) for analytical purposes were carried out on silica gel and developed. Benzidine, ninhydrin, and hydroxamate tests used for detection reactions. The IR spectra of the compounds were recorded on a Perkin–Elmer spectrophotometer model 1430 as potassium bromide pellets and frequencies are reported in  $\text{cm}^{-1}$ . The mass spectra were recorded on a mass spectrometer HP model MS–QPL000EX (Shimadzu) at 70 eV. Elemental analyses (C, H, and N) were carried out at the Micro analytical Centre of Cairo University, Giza, Egypt.

### 2-(7-hydroxy-2-oxo-2H-chromen-4-yl)acetyl chloride(2)

The starting material (2) was prepared as mentioned earlier [17], respectively.

### (2-(7-hydroxy-2-oxo-2H-chromen-4-yl)acetyl)alanine (4)

White crystals. In 72% yield RF = 0.84 (Toluene/MeOH=3/1); M.P. = 140-142°C; IR (KBr  $\text{cm}^{-1}$ )  $\nu$ ; 3396 broad band due to overlapping (NH, OH), 2958(CH-ali), 1722, 1665 (C=O) and 1621(CONH); Anal. /Calcd. For  $\text{C}_{14}\text{H}_{13}\text{NO}_6$  (291): C (57.71%), H (4.46%), and N (4.80%). Found: C (57.72); H (4.51); N, (4.81).

General procedure for synthesis of (2-(7-hydroxy-2-oxo-2H-chromen-4-yl)acetyl)-alanylglycine (8)

### Method 1

A mixture of compound (1; 0.01 mol) was fused at 160°C in an oil bath for 40 mins. The fused mass was dissolved in ethanol and poured onto cold water; the solid obtained was recrystallized from ethanol to give compound (3).

### Method 2

The  $\beta$ -alanine (0.01 mol.) was dissolved in a mixture (water (25ml), THF (15ml) and triethylamine (2 ml)), acid chloride (5; 0.01 mmol) was added to reaction mixture during 30 mins; temperature of the reaction mixture was kept at 10°C during the addition. Stirring was continued for 3 hrs. THF was removed under reduced pressure; water (30 ml) was added and acidified with 1 N HCl to pH = 5. The crude product was filtered and recrystallized from ethanol.

Yellow crystal in yield (75 %);  $R_f = 0.84$  (Toluene /MeOH=3/1); M.P= 162-164°C; IR  $\nu$ : 3399 broad band overlapping (NH, OH), 3035 ( $\text{CH}_{\text{-arm}}$ ) 2959 ( $\text{CH}_{\text{-ali}}$ ), 1621 (CONH)  $\text{cm}^{-1}$ ; Anal. /Calcd. for  $\text{C}_{16}\text{H}_{16}\text{N}_2\text{O}_7$  (348): C (55.17%), H (4.59%), N (8.04%). Found: C (55.15); H (4.63); N, (8.04).

### Synthesis Methyl (2-(7-hydroxy-2-oxo-2H-chromen-4-yl) acetyl) $\beta$ -laminic acid (5):

The free amino acid derivatives (3; 0.01 mol) in absolute methanol (50ml) were cooled to 0-5°C, pure thionyl chloride (0.015 mmol) was added drop wise during one hour. The reaction mixtures were stirred for an additional 3 hrs. At room temperature, and kept overnight. The solvents were removed by vacuum distillation, the residue also lids were recrystallized from ethanol. The product 5 chromatographically homogeneous by iodine and Benzidine development. Yellowish brown crystal: yields=70%;  $R_f = 0.79$  ( $\text{CHCl}_3/\text{EtOH}=3/1$ ); mp: 116-118°C; IR ( $\text{KBr cm}^{-1}$ )  $\nu$ : 3396 broad band (OH+ NH + $\text{CH}_{\text{-arom}}$ ), 2959 ( $\text{CH}_{\text{-ali}}$ ), 1693 (CO)  $\text{cm}^{-1}$ ; Anal. /Calcd. For  $\text{C}_{15}\text{H}_{15}\text{NO}_6$  (305): C (58.99 %), H (4.91%), N (4.58%). Found: C (59.01); H (4.95); N, (4.59).

### Synthesis of 2-(2-((7-hydroxy-2-oxo-2H-chromen-4-yl)methyl)-4-oxoquinazolin-3(4H-yl)propanehydrazide(7)

$\beta$ -alaninyl methyl ester derivatives (5; 0.01 mol) was dissolved in ethanol (100ml) and 85 % hydrazine hydrate (6.3 ml), the mixtures were refluxed for 30 mins., left overnight at 25°C. The products were separated, and collected by filtration, washed with methanol and light petroleum ether, and recrystallized from ethanol to give desired hydrazid derivatives (6). White crystal (6) yields (78 %); positive ninhydrin spots of  $\beta$ -Ala. (acid hydrolysis (6N-HCl) at 110 °C for 24 hrs);  $R_f = 0.72$  (Toluene /MeOH=3/1); M.P= 158-160°C;  $\nu$ : 3401 broad band overlapping of (OH+  $\text{NH}_2$ +NH+ $\text{CH}_{\text{-arom}}$ ), 2958 ( $\text{CH}_{\text{-ali}}$ ), 1636 (CONH)  $\text{cm}^{-1}$ ; Anal./Calcd. for  $\text{C}_{21}\text{H}_{18}\text{N}_4\text{O}_5$  (406): C (62.04%), H (4.43%), N (13.79%). Found: C (62.07); H (4.46); N, (13.79).

## Molecular Modeling Study

### Computational Model

All the Quantum chemical computations were performed, using the PM3 semi-empirical Hamiltonian molecular orbital calculation MOPAC16 package [18], then employing density function theory in Gaussian 09W program package [40] with the Becke3-Lee-Yang-parr (B3LYP) level using 6-311G\* basis as implemented in MOE 2015 package [19]. The optimization Geometry for molecular structures was carried out, for improve knowledge of chemical structures.

### Generation of Ligand and Enzyme Structures

### Preparation of Small Molecule

Molecular modeling of the target compounds were built using MOE 2015, and were minimized their energy with PM3 through MOPAC then DFT using B3LYP/6-311G. Our compounds were introduced into the binding sites according to the published crystal structures.

### Selection of COX-2 structures

Docking experiment was carried out for the target active site into COX-2 (ID: 1PXX[34]) using MOE 2015[19]. The crystal structures of the (COX-2) complexes with (**diclofenac**).

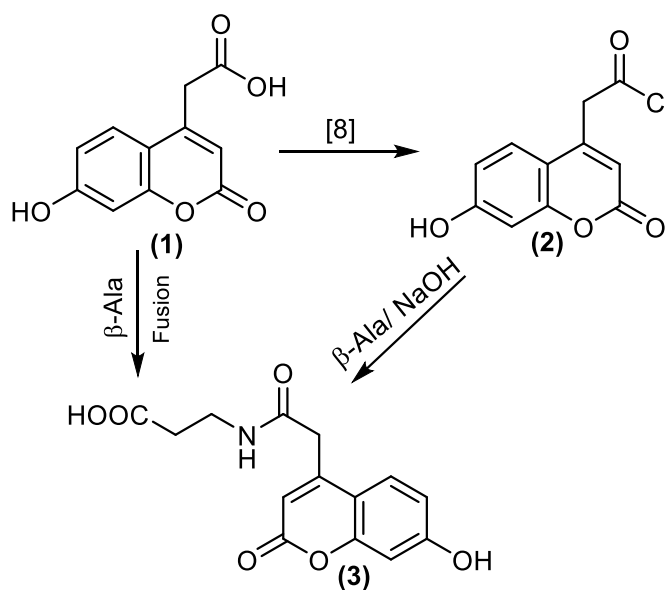
### MOE Stepwise Docking Method

The crystal structures of the (COX -2) complexed with reference inhibitor **diclofenac** was obtained. Water and inhibitors molecule were removed, and hydrogen atoms were added. The parameters and charges were assigned with MMFF94x force field. After alpha-site spheres were generated using the site finder module of MOE. The optimized 3D structures of molecules were subjected to generate different poses of ligands using triangular matcher placement method, which generating poses by aligning ligand triplets of atoms on triplets of alpha spheres represented in the receptor site points, a random triplet of alpha sphere center was used to determine the pose during each iteration. The pose generated was rescored using London dG scoring function. The poses generated were refined with MMFF94x force field; also, the salvation effects were treated. The Born salvation model (GB/VI) was used to calculate the final energy, and the finally assigned poses were assigned a score based on the free energy in kcal/mol.

## RESULTS AND DISCUSSION

### Chemistry

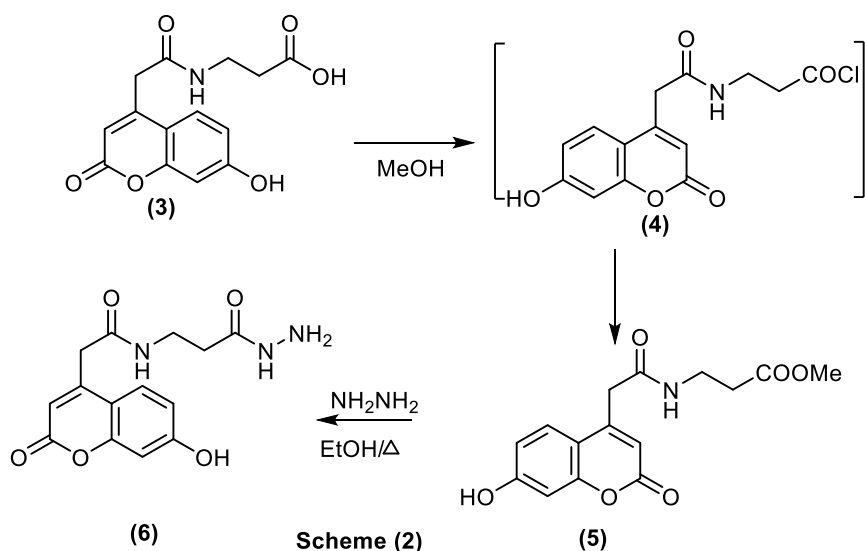
The starting acid chloride **2** was carried out according to reported earlier[17], which was reacted with with  $\beta$ -alanine ( $\beta$ -Ala.), to afford free acid derivative **3** (Scheme 1). The appearance of characteristic NH bands; of IR spectra at 3212 and 3396 $\text{cm}^{-1}$ , and molecular ion peak which supported the proposed structure.



Scheme(1)

Scheme 1: Synthesis of compounds ( 1-3).

The free acid derivative **3** was methylated to corresponding methyl ester derivative **5** via acid chloride synthesis, the compound **5** was reacted with alcoholic hydrazine to form hydrazide **6**, which showed molecular ion peak at (305m/z)(Scheme2).



**Scheme 2: Synthesis of compounds (4-6).**

### Molecular Modeling Studies

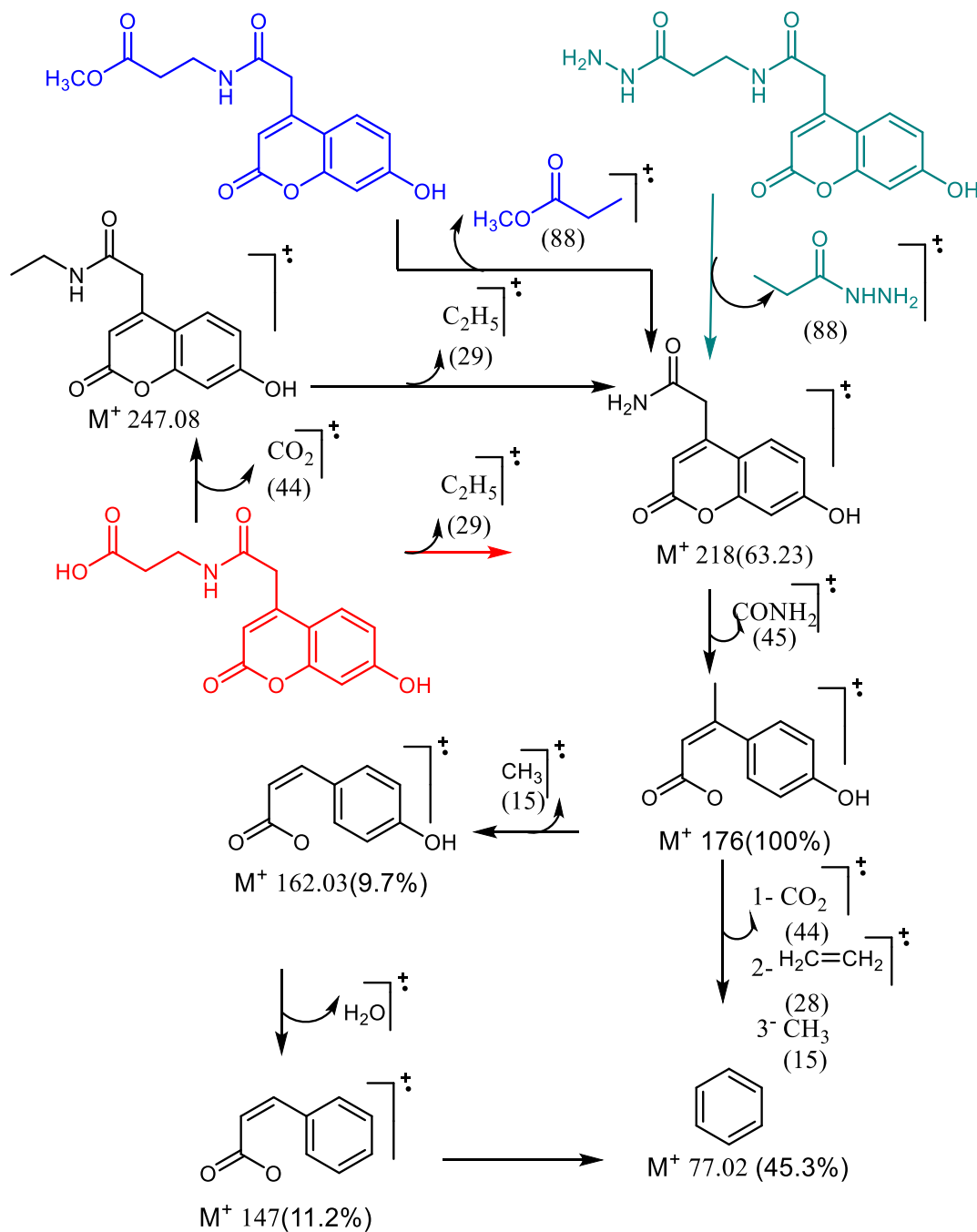
#### Molecular Geometry

The single crystal cannot be obtained till now, thus, the optimization geometries and conformational analysis were performed, for isolated synthesized compounds (**3**, **5** and **6**), using the PM3 semi-empirical Hamiltonian molecular orbital calculation MOPAC16 package [18], then using density function theory in Gaussian 09 package as implemented in MOE 2015 [19], which considering important guide tool for preferring the most stable stereoisomer forms for target compounds, all calculated energies were summarized in (table 1).

The fully optimization geometry for studied ligands (**3**, **5** and **6**) exhibited, its compounds were stabilized by adjusting the benzocoumarin rings with  $\beta$ -Ala fragments in planner and coplanar for all ligands (Figure 1). The compounds (**3**) exhibited smaller bond length of C19—O<sub>20</sub> (1.353 Å) than CO at C19—O<sub>20</sub>, for compounds **5** (1.357Å) and C19—N<sub>20</sub> (1.471 Å) respectively, this may explained by presence releasing fragment (CH<sub>3</sub>) in **6**, that pull electrons toward carbon of carbonyl and length bond.

#### Frontier Orbital Analysis

The “FMOs” frontier molecular orbital’s, which defined as HOMO (donating electron) and LUMO (accepting electron), which are a vital orbital for molecules, that can be decide the interaction rout with receptor. The “simple Hackle Molecular Orbital theory (SHMO)” used for determine FMOs gap, which lead to characterize the chemical reactivity and kinetic stability of the molecule[20]. The higher energies for **HOMO** showed, the strong ability molecule for electron donating, and led to lose interaction electron valance, susceptible to oxidation, and *vis versa*[21, 22]. The **HOMOs** and **LUMOs** were studied in the S<sub>0</sub>, the E<sub>HOMO</sub> are arranged in decreasing order **6** > **5** > **3** (Figure2).



**Scheme 3: Mass fragmentation pattern of (4-6).**

The transition of HOMO→LUMO suggested the electron flow from alaninyl fragment to pyran ring. The negative values of  $\Delta G$ , exhibited the non-linear optical (NLO) activity for all compounds[23]. The low value FMOs of the synthesized compounds (3,5 and 6), lead to more reactive and less stable for its compounds. In addition, the HOMO drug is interacted with the LUMO receptor and vice versa, the binding interactions are stabilized inversely with energy gap, the increasing HOMO energy receptors and decreasing LUMO energy in the drug molecule lead to enhancement stabilizing interactions with receptor [21].

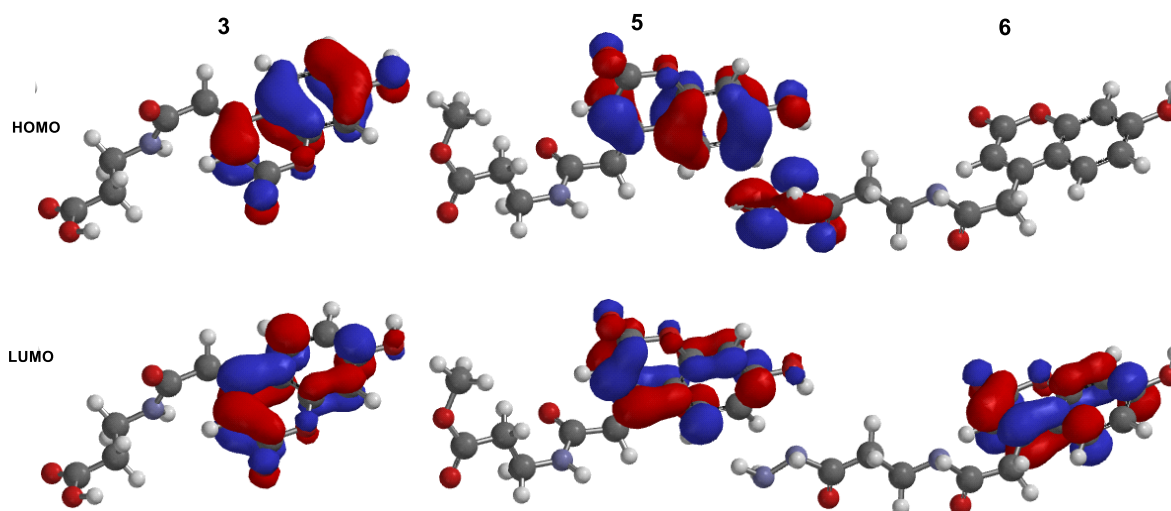


Figure 2: plotting HOMO and LUMO molecular orbital for compounds (3, 5 and 6).

### Inter- and Intermolecular Interaction of Synthesized Compounds (3, 5 and 6) and COX-2 Receptor in global Electronic Descriptor Terms

The global chemical reactivity descriptors for molecules have been computed (table 1), like;  $S$ ; softness (measures stability of molecules and chemical reactivity with direct proportional [24]),  $\eta$ ; hardness (reciprocal of softness),  $\mu$ ; chemical potential,  $\chi$ ; electro negativity (strength atom for catching electrons), [25-29]. Also computed, the chemical potential gain for:  $\mu^-$ ; electron donating, and  $\mu^+$ ; electro accepting, measuring powers of  $\omega^-$ ; electro donating, and  $\omega^+$ ; electro accepting,  $\omega^\pm$ ; net electrophilicity (measuring relative powers between electron accepting and electron donating) [26],  $\omega_i$ ; Electrophilicity index in ground state (determining decreasing energy obtained from maximal movement electrons current between donor and acceptor),  $\omega_i^{VS}$ ; Electrophilicity index in valance state [25]. These parameters are represented in terms of the  $I$ ; ionization potential (total energy variance, when losing electron ( $N - 1$ ) from the same molecule ( $N$ ) electrons at a fixed outer electron potential), and the  $A$ ; electron affinity (determined accepting electron ( $N + 1$ ) at the same conditions [26], where  $u(r)$  are external potential of an  $N$ -electron system, the previous terms represented in (Equation 1-11).

$$\eta = 1/2[\partial^2 E / \partial^2 N^2]_{u(r)} = 1/2[\partial E / \partial N^2]_{u(r)} \quad \text{equation (1)}$$

$$S = 1/\eta \quad \text{equation (2)}$$

$$\mu = [\partial E / \partial N]_{u(r)} \quad \text{equation (3)}$$

$$\chi = -\mu = -[\partial E / \partial N]_{u(r)} \quad \text{equation (4)}$$

$$\mu^- = -1/4(3I + A) \quad \text{equation (5)}$$

$$\mu^+ = -1/4(I + 3A) \quad \text{equation (6)}$$

$$\omega^- = -(3I + A)^2 / 16(I - A) \quad \text{equation (7)}$$

$$\omega^+ = (3I + A)^2 / 16(I - A) \quad \text{equation (8)}$$

$$\omega^\pm = \omega^+ + \omega^- \quad \text{equation (9)}$$

$$\omega_i = \mu^2 / 2\eta \quad \text{equation (10)}$$

$$\omega_i^{VS} = (I + A)^2 / 4(I - A) \quad \text{equation (11)}$$

Table 1: Calculated energetic global reactivity parameters for compounds (3, 5 and 6) at DFT with a B3LYP\6-31G\* Basics sets. 758114103

Cpd.	3	5	6
E	-82129.4297	-84840.6172	-82857.1563
Eele	-457169.813	-497156.5	-507100.813
Esol	-18.6223793	-8.42055607	-7.7405076
HF	-834.426	-805.587	-339.465
HOMO	-9.63	-9.56	-9.29

LUMO	-1.01	-1.11	-1.42
$\Delta G$	-8.62	-8.45	-8.87901
I	9.63	9.56	9.29
A	1.01	1.11	0.41099
$\eta$	4.31	4.225	4.439505
S	0.232019	0.236686	0.22525
$\chi$	-5.32	-5.335	-4.8505
$\omega_i$	3.283341	3.368311	2.649766
$\mu^+$	-3.165	-3.2225	-2.63074
$\mu^-$	-7.475	-7.4475	-7.07025
$\omega^-$	6.482091	6.563936	5.629952
$\omega^+$	2.744591	2.840186	2.094828
$\omega^{+-}$	9.226682	9.404121	7.72478
$\Delta N_{max}$	-0.61717	-0.63136	-0.54629
$\Delta E_{max}^{GS}$	1.234339	1.262722	1.092576
$\Delta E_{max}^{VS}$	2.468677	2.525444	2.185151

E: The total energy (kcal/mol), E-ele: electrostatic energy (kcal/mol), E-sol: Solvation energy (kcal/mol), HF: heat of formation (kcal/mol), HOMO: Highest Occupied Molecular Orbital (eV), LUMO: Lowest Occupied Molecular Orbital (eV),  $\Delta G$ : difference between HOMO and LUMO energy levels (eV), I: Ionization potential, A; electron affinity;  $\eta$ : Hardness (eV), S: Softness (eV),  $\chi$ : Electro negativity (eV),  $\omega_i$ : electrophilicity index;  $\mu^+$ : electron accepting chemical potentials,  $\mu^-$ : electron donating chemical potentials,  $\mu$ : chemical potential (eV),  $\omega^+$ : electron accepting,  $\omega^-$ : Electro donating power;  $\omega^{+-}$ : Electrophilicity (eV);  $\Delta N_{max}$ : maximum number of electrons transfer;  $\Delta E_{max}^{GS}$ : maximum number of electrons transfer in ground state;  $\Delta E_{max}^{VS}$ : maximum number of electrons transfer in valance state.

The reactivity index measures the stabilization in energy when the system acquires an additional electronic charge " $\Delta N_{max}$ " from the environment. So, the charge transfer is examined (table 1), as  $\Delta N_{max} = \chi/2\eta$  (maximum number of electrons transferred during a chemical reaction); " $\Delta E_{max}^{GS}$ " (maximal electron transfer lead to lowering of the total binding energy in ground state, and computed as  $(I + A)/(I - A)$ ), " $\Delta E_{max}^{VS}$ " is a maximal electron transfer in valance state, that represented as  $\Delta E_{max}^{VS} = 2 \Delta E_{max}^{GS}$ .

The electrophiles and nucleophiles have been described with soft and hard terms, which direct related with FOMs energies, increasing FMOs energies related with soft nucleophiles and hard electrophiles. The  $\Delta G$  has been used as a stability index measurement, the molecule with small energy gap is high polarizability, softness, chemical reactivity and nucleophilicity (easily offer electrons to an acceptor), and vice versa. It was observed that (table 1); all compounds (**3**, **5** and **6**) have low softness values in ranged, which lead to high reactivity against biological environment (Table 1).

The methyl ester derivative **5** showed better values for " $\mu^+$ ,  $\omega^-$ ,  $\omega^+$   $\omega_i$  and  $\omega^{+-}$ " than other compounds **3** and **6**.

### Molecular Electrostatic Potential (MEP)

The molecular electrostatic potentials (MEP) was drawn (Figure 3), for synthesized compounds (**3**, **5** and **6**). The MEP is represents a balance between repulsive interactions of the nuclei (positively charge which related to nucleophilic reactivity) and attractive interactions for the electrons (negatively charge are related to electrophilic reactivity). The colors toward (orange, yellow, and red) depict negative potential (high electron density area), while colors toward blue depict positive potential, and color (green) depict intermediate values of the potential. The negative charge covers carbonyl groups and oxygen tom of coumarin, which positive charge lying upon alanyl moiety of amino acid. The color variation in MEP surface, exhibited the difference at electrostatic potential value, increasing red region related to electrophilic potency of the compounds. The substrate-receptor interaction, frequently obtained from potential electrostatic values, its responsible for reorganization substrate with binding site receptors [30].

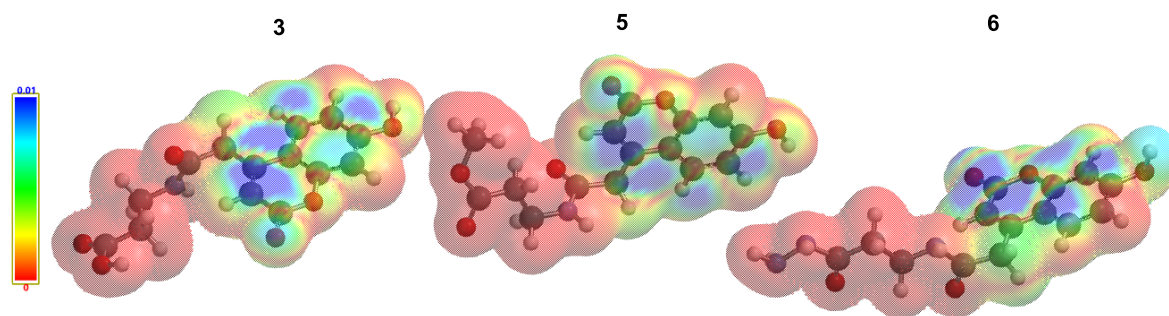


Figure 3: MEP plot of synthesized compounds (3, 5 and 6)

Table 2: Calculated thermodynamic parameters for compounds (3, 4, 6-8, 10 and 11) at DFT with a B3LYP\6-31G\* Basics sets.

Cpd.	3	5	6
ZPE	669.447	736.566	738.47
H°	0.045	0.712	0.170
G°	0.105	0.0715	0.107
S°	34.985	550.410	553.99
C <sub>v</sub> °	201.617	213.155	239.22
μ <sub>x</sub>	2.078763	2.1452	-0.502
μ <sub>y</sub>	-1.855815	1.418	-2.382
μ <sub>z</sub>	0.786431	0.8673	2.337
μ	7.35903	6.8976	8.580
α <sub>xx</sub>	197.986	207.4107	215.715
α <sub>yy</sub>	164.3522	173.8168	160.028
α <sub>zz</sub>	68.447	74.37121	95.007
α <sub>xz</sub>	27.472	26.87373	43.327
α <sub>xy</sub>	27.472	13.0548	-21.534
α <sub>yz</sub>	-10.0868	8.632064	-12.311
α <sub>0</sub>	79.273	84.02655	80.03867
Δα	4.255	4.500	4.650
β <sub>xxx</sub>	388.969	405.915	-241.552
β <sub>xyy</sub>	102.566	-109.109	101.479
β <sub>xzz</sub>	54.575	-58.7	63.941
β <sub>yyy</sub>	53.471	-39.549	23.708
β <sub>xyx</sub>	-77.763	46.73	-18.447
β <sub>yyz</sub>	5.286	-1.538	44.969
β <sub>zzz</sub>	30.033	34.829	22.588
β <sub>xyz</sub>	80.395	82.942	99.619
β <sub>yyz</sub>	-22.067	-26.548	-18.994
β <sub>0</sub>	12.052	11.44	24.6

**ZPE:**

zero-point vibrational energies(kj/mol),, **H°**: Enthalpy (kj/mol), **G°**: Gibbs free energy (kj/mol), **S°**: Entropy (kj/mol), **C<sub>v</sub>°**: Constant volume molar heat capacity, **μ**: dipole moment (Deby), **α<sub>0</sub>**: mean polarizability(x10<sup>-30</sup>esu), **Δα**: anisotropic polarizability(x10<sup>-30</sup>esu), **β<sub>0</sub>**: hyperpolarizability(x10<sup>-30</sup>esu).

**Nonlinear optical effects**

The “**μ**”dipole moments (determine ability electrostatic interaction of the molecule with media), “**α**”polarizability (measurement deformation degree for electron density, its parameter based on geometrical

and bonding nature for the molecules), “ $\alpha_0$ ” mean polarizability, “ $\Delta\alpha$ ” anisotropic polarizability and “first order hyperpolarizability were calculated against to  $x$ ,  $y$  and  $z$  polarizability tensors.

$$\begin{aligned} \mu &= (\mu_x^2 + \mu_y^2 + \mu_z^2)^{1/2} \\ \alpha &= 1/3 (\alpha_{xx}^2 + \alpha_{yy}^2 + \alpha_{zz}^2) \\ \alpha_0 &= 2^{-1/2} [(\alpha_{xx} - \alpha_{yy}) + (\alpha_{yy} + \alpha_{zz}) + (\alpha_{zz} + \alpha_{xx}) + \alpha]^2 \\ \beta_0 &= (\beta_{xx}^2 + \beta_{yy}^2 + \beta_{zz}^2)^{1/2} \\ \beta_x &= (\beta_{xxx} + \beta_{xyy} + \beta_{xzz}) \\ \beta_y &= (\beta_{yyy} + \beta_{xxy} + \beta_{yzz}) \\ \beta_z &= (\beta_{zzz} + \beta_{xxz} + \beta_{yzz}) \end{aligned}$$

Urea is used as standard NLO material with  $\mu$ (1.3732 Debye) and  $\alpha$  (0.3728 x 10<sup>-30</sup>esu.)[31], the compound hyperpolarizability of the synthesized compounds **5** more than other compounds **3** and **6**, all members **3**, **5** and **6** more than **urea**(table 2). These data showed that, the intermolecular charge transfer take place, from electron donating to electron accepting groups via  $\pi$ -electron systems[32]. These results indicate that, the synthesized compounds (**3,5**and**6**) have been a promising NLO material against standard material.

### 2.3. Docking Studies

The X-ray analysis of COX-2 active site showed that, the carboxyl group of arachidonic acid was coordinated with Tyr385 and Ser-530 through tetrahedral intermediate, which stabilized by negative charge [33, 34]. The NSAIDs inhibit COX-2 with the same manner of arachidonic acid[35]. Thus, the Tyr-385 and Ser-530 have vital structural and functional site for chelating ligand [34]. In order to rationalized biological data on a structural basis through ligand–protein interaction behavior.

**Table 3: Pharmacokinetic parameters and Docking energy scores (kcal/mol) derived from the MOE for ligands (3, 4, 6-8, 10 and 11).**

Cpd.	3	5	6
dig	-29.23	-110.757	-13.0140
Int	-79.03	-107.513	-118.36
H.B	-8.036	-118.056	-4.583
HBD	3	2	2
HBA	7	7	5
Log.P	0.63	0.89	0.310
V	0	0	0
Drug like	1	1	1
TPSA	112.93	101.93	130.36
%ABS	70.039	73.834	63.891
Log.S	-2.35089	-2.76322	-2.61354
Vol.	121.5	134.125	127.25
Mutagenic	0	0	0

### d.G:

Free binding energy of the ligand from a given conformer, **Int.**: Affinity binding energy of hydrogen bond interaction with receptor, **H.B.**: Hydrogen bonding energy between protein and ligand. **Eele**: Electrostatic interaction with the receptor, **Evdw**: Van der Waals energies between the ligand and the receptor. **HBD**: Number of hydrogen bond donor, **HBA**: Number of hydrogen bond acceptor, **Log P**: Calculated Lipophilicity. **V**: Number of violation from Lipinski’s rule of five, **Log S**: Solubility parameter, **TPSA**: Polar surface area (Å<sup>2</sup>), **%ABS**: Absorption percentage, **Vol**: Volume (Å<sup>3</sup>).

All calculations for docking experiment preformed with MOE 2015.10[19]. The tested compounds were evaluated in silico (table 3), using X-ray crystal structure of COX-2 (ID: 1PXX[34]) complex with reference inhibitor[33]. The tested compounds (**3**, **5** and **6**) were docked into COX-2 active site. The binding affinity for complexes (inhibitor-COX-2) was performed through MOE scoring function of the most stable docking model of ligands. The complexes were energy-minimized with an MMFF94 force field[36] until the gradient convergence 0.05 kcal/mol. reached. The compounds (**3**, **4**, **6-8**, **10** and **11**) docked successfully into the COX-2 active site, and compared with reference inhibitor (diclofenac). In order to get a deeper insight into the nature and type of interactions of docked compounds **3**, **5** and **6**, the complexes between (Ligand-COX-2 receptor) were visualized and depicted in (Figures4). The inhibition potency for compounds were arranged as **3** < **6** < **5** with binding score values in ranged about ( $\sim$  dG = - 107 – 118Kcal/mol.). The compound **3** was occupied binding pocket by adjusting phenyl ring of Tyr-385 and coumarin ring in Parallel mode. (Figure.4). The results obtained clearly revealed that, the amino acid residues close to the reference molecules are mostly the same as observed in the tested compounds under (Figures 4).

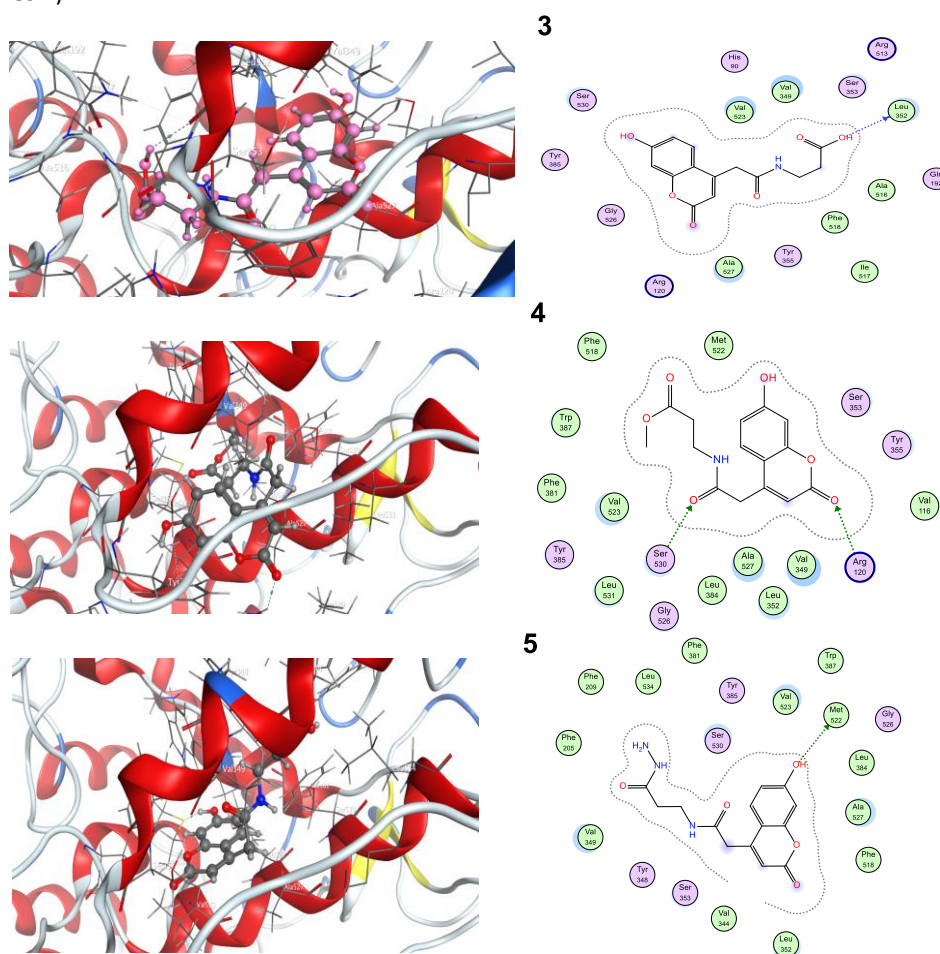


**Figure 4: The most active compound 3, 5, and 6 were Docked into the active site of COX-2, using MOE tool, H- bonds are in blue.**

The highest binding process interaction observed in **3** with COX-2, which indicated that, the compound **3** act as selective inhibitors against COX-2, this could probably due to the presence of hydrophobic amino acid in the synthesized compounds.

#### ADMET Profile

The Oral bioavailability is acting a vital role in the enhance menta therapeutic bioactive molecules. The ADMET Factors are prevented several powerful a therapeutic agent to use in the clinic filed. Thus, ADMET properties of the molecules was performed for isolated compounds (**3,4,6-8**, **10** and **11**),through calculated

Lipinski rules [37], percent absorption (%ABS) [38], and topological polar surface area (TPSA), which linked to drug bio availability, the passively absorbed molecules with (TPSA>140) have low or albio availability [39]. All calculated descriptors were performed using MOE Package [49], and their results were disclosed in (Table 3). The tested compounds showed, the (5-7) values for H-bond acceptors, the H-bond donors in ranged between 2 and 3, the "Clog P" lipophilicity characters is lower than 5.0 [39]. These compounds fulfill Lipinski's rule. Also, the absorption percent in ranged between (~ 63-73%).

## CONCLUSIONS

The present work aims to synthesis some novel NASIDS containing coumarin nucleus. The synthesized compounds were characterized by different spectral data. The optimization geometries for compounds 3, 5 and 6. The FMO, thermodynamic parameters, and MEP were calculated, which showed that the electron flow from alaninyl fragment to pyran ring. The global and local reactivity: Fukui function index, local electrophilicity and softness were performed, which to be a helpful tool to predict a possible explanation for chemical reactivity of ligand, this data indicated the methyl ester derivative 5 is the best electrophile. The NLO properties for the synthesized compounds 3, 5 and 6 have been a promising NLO material, due to, the intermolecular charge transfer take place from electron donating to electron accepting groups via  $\pi$ -electron systems. The molecular docking simulations into the active site of COX-2 showed that, compounds 3, 5 and 6 suitable inhibitor against COX-2, and can used as new class of NSAIDs. The ADMET profiles in silico showed that, these compounds are good oral bioavailability.

## REFERENCES

- [1] Nair, B. and R. Taylor-Gjevre, A review of topical diclofenac use in musculoskeletal disease. *Pharmaceuticals*, 2010. **3**(6): p. 1892-1908. <http://www.mdpi.com/1424-8247/3/6/1892/pdf>.
- [2] Gabriel, S.E. and E.L. Matteson, Economic and Quality-of-Life Impact of NSAIDs in Rheumatoid Arthritis. *Pharmacoeconomics*, 1995. **8**(6): p. 479-490.
- [3] Zochling, J., et al., Nonsteroidal anti-inflammatory drug use in ankylosing spondylitis—a population-based survey. *Clinical rheumatology*, 2006. **25**(6): p. 794-800.
- [4] Hall, J.E., Guyton and Hall Textbook of Medical Physiology E-Book. 2015: Elsevier Health Sciences.
- [5] Vane, J.R., Y.S. Bakhle, and R.M. Botting, Cyclooxygenases 1 and 2. *Annu Rev Pharmacol Toxicol*, 1998. **38**(1): p. 97-120. doi:10.1146/annurev.pharmtox.38.1.97, <https://www.ncbi.nlm.nih.gov/pubmed/9597150>.
- [6] Guslandi, M., Gastric toxicity of antiplatelet therapy with low-dose aspirin. *Drugs*, 1997. **53**(1): p. 1-5. <https://www.ncbi.nlm.nih.gov/pubmed/9010645>.
- [7] Mazumdar, K., et al., Diclofenac in the management of E. coli urinary tract infections. *in vivo*, 2006. **20**(5): p. 613-619.
- [8] Bhandari, S.V., et al., Design, synthesis and evaluation of antiinflammatory, analgesic and ulcerogenicity studies of novel S-substituted phenacyl-1, 3, 4-oxadiazole-2-thiol and Schiff bases of diclofenac acid as nonulcerogenic derivatives. *Bioorganic & medicinal chemistry*, 2008. **16**(4): p. 1822-1831.
- [9] Amir, M. and K. Shikha, Synthesis and anti-inflammatory, analgesic, ulcerogenic and lipid peroxidation activities of some new 2-[(2, 6-dichloroanilino) phenyl] acetic acid derivatives. *European Journal of Medicinal Chemistry*, 2004. **39**(6): p. 535-545.
- [10] Elhenawy, A., M. El-Gazzar, and A. Seliem, Discovery potent of Novel Naproxen Derivatives Containing  $\beta$ -Alanyl Moiety. *Global Journal of Chemistry*, 2015. **2**(1): p. 45-50.
- [11] Sidhu, R.S., et al., Comparison of cyclooxygenase-1 crystal structures: cross-talk between monomers comprising cyclooxygenase-1 homodimers. *Biochemistry*, 2010. **49**(33): p. 7069-7079. <https://www.ncbi.nlm.nih.gov/pmc/articles/PMC2932651/pdf/nihms-223818.pdf>.
- [12] Goto, M., et al., Antiinflammatory Activity of N-Naphthoyl D-Alanine in vivo. *ChemInform*, 2009. **40**(37): p. i.
- [13] Sajadi, Z., et al., Antitumor and antiinflammatory agents: N-benzoyl-protected cyanomethyl esters of amino acids. *Journal of medicinal chemistry*, 1979. **22**(11): p. 1419-1422.
- [14] Al-Omar, M.A. and A.E.-G.E. Amr, Synthesis of some new pyridine-2, 6-carboxamide-derived Schiff bases as potential antimicrobial agents. *Molecules*, 2010. **15**(7): p. 4711-4721.
- [15] Maresca, A., et al., Deciphering the mechanism of carbonic anhydrase inhibition with coumarins and thiocoumarins. *Journal of medicinal chemistry*, 2009. **53**(1): p. 335-344.

- [16] Maresca, A., et al., Non-Zinc Mediated Inhibition of Carbonic Anhydrases: Coumarins Are a New Class of Suicide Inhibitors#. *Journal of the American Chemical Society*, 2009. **131**(8): p. 3057-3062. <http://pubs.acs.org/doi/abs/10.1021/ja809683v>.
- [17] Mona S. Kadah, A.A.E., Reda D. Abd – Elghany, M. K. Hassanein, Design and Synthesis of Novel NSAIDs Class Acting as Anticancer Agents. *International Journal of Sciences: Basic and Applied Research*, 2016. **30**(4): p. 32-52.
- [18] Stewart, J.J., MOPAC manual. Constraints, 1993. **3**: p. 2.
- [19] Molecular Operating Environment (MOE), C.C.G.U., 1010 handbook St. West, Suite 910, Montreal, QC, Canada, H3A 2R7, 2017.
- [20] Hofmann, P., Arvi Rauk: "Orbital Interaction Theory of Organic Chemistry" Wiley & Sons: New York 1994. ISBN 0-471-59389-3. 307 Seiten, mit HMO-Programmdiskette, Preis: \$45.50. *Berichte der Bunsengesellschaft für physikalische Chemie*, 1995. **99**(8): p. 997-999.
- [21] Fukui, K., Role of frontier orbitals in chemical reactions. *Science*, 1982. **218**(4574): p. 747-54. doi:10.1126/science.218.4574.747, <https://www.ncbi.nlm.nih.gov/pubmed/17771019>.
- [22] Wildman, S.A. and G.M. Crippen, Prediction of physicochemical parameters by atomic contributions. *Journal of chemical information and computer sciences*, 1999. **39**(5): p. 868-873.
- [23] Handy, N.C., et al., The harmonic frequencies of benzene. *Chemical physics letters*, 1992. **197**(4-5): p. 506-515.
- [24] Parr, R.G. and P.K. Chattaraj, Principle of maximum hardness. *Journal of the American Chemical Society*, 1991. **113**(5): p. 1854-1855.
- [25] Parr, R.G., L.v. Szentpaly, and S. Liu, Electrophilicity index. *Journal of the American Chemical Society*, 1999. **121**(9): p. 1922-1924.
- [26] Lamaka, S.V., et al., Nanoporous titania interlayer as reservoir of corrosion inhibitors for coatings with self-healing ability. *Progress in organic coatings*, 2007. **58**(2): p. 127-135.
- [27] Mendoza-Huizar, L.H. and C.H. Rios-Reyes, Chemical reactivity of atrazine employing the Fukui function. *Journal of the Mexican Chemical Society*, 2011. **55**(3): p. 142-147.
- [28] Komorowski, L., et al., Polarization justified Fukui functions: the theory and applications for molecules. *J Chem Phys*, 2011. **135**(1): p. 014109. doi:10.1063/1.3603449, <https://www.ncbi.nlm.nih.gov/pubmed/21744890>
- [29] Eddy, N.O., et al., Experimental and computational chemistry studies on the inhibition of the corrosion of mild steel in H<sub>2</sub>SO<sub>4</sub> by (2s, 5s, 6r)-6-(2-(aminomethyl)-5-(3-(2-chlorophenyl) isoxazol-5-yl) benzamido)-3, 3-dimethyl-7-oxo-4-thia-1-azabicyclo [3.2. 0] heptane-2-carboxylic acid. *Int. J. Electrochem. Sci*, 2011. **6**: p. 4296-4315.
- [30] Luque, F.J., J.M. López, and M. Orozco, Perspective on "Electrostatic interactions of a solute with a continuum. A direct utilization of ab initio molecular potentials for the prevision of solvent effects", in *Theoretical Chemistry Accounts*. 2000, Springer. p. 343-345.
- [31] Adant, C., M. Dupuis, and J. Bredas, Ab initio study of the nonlinear optical properties of urea: Electron correlation and dispersion effects. *International Journal of Quantum Chemistry*, 1995. **56**(S29): p. 497-507.
- [32] Abraham, J.P., et al., Efficient  $\pi$ -electron conjugated push-pull nonlinear optical chromophore 1-(4-methoxyphenyl)-3-(3, 4-dimethoxyphenyl)-2-propen-1-one: A vibrational spectral study. *Journal of Molecular Structure*, 2009. **917**(1): p. 27-36.
- [33] Kiefer, J.R., et al., Structural insights into the stereochemistry of the cyclooxygenase reaction. *Nature*, 2000. **405**(6782): p. 97.
- [34] Rowlinson, S.W., et al., A novel mechanism of cyclooxygenase-2 inhibition involving interactions with Ser-530 and Tyr-385. *J Biol Chem*, 2003. **278**(46): p. 45763-9. doi:10.1074/jbc.M305481200, <https://www.ncbi.nlm.nih.gov/pubmed/12925531>
- [35] Hochgesang, G.P., S.W. Rowlinson, and L.J. Marnett, Tyrosine-385 Is Critical for Acetylation of Cyclooxygenase-2 by Aspirin. *Journal of the American Chemical Society*, 2000. **122**(27): p. 6514-6515. doi:10.1021/ja0003932, <http://dx.doi.org/10.1021/ja0003932>
- [36] Halgren, T.A., Merck molecular force field. I. Basis, form, scope, parameterization, and performance of MMFF94. *Journal of computational chemistry*, 1996. **17**(5-6): p. 490-519.
- [37] Lipinski, C.A., et al., Experimental and computational approaches to estimate solubility and permeability in drug discovery and development settings. *Advanced drug delivery reviews*, 1997. **23**(1-3): p. 3-25.
- [38] Zhao, Y.H., et al., Rate-limited steps of human oral absorption and QSAR studies. *Pharm Res*, 2002. **19**(10): p. 1446-57. <https://www.ncbi.nlm.nih.gov/pubmed/12425461>.



- [39] Clark, D.E. and S.D. Pickett, Computational methods for the prediction of 'drug-likeness'. *Drug discovery today*, 2000. **5**(2): p. 49-58.
- [40] Frisch, M., et al., Gaussian 09, Revision D. 01, Gaussian, Inc., Wallingford CT. Gaussian 09, Revision D01, Gaussian. Inc, Wallingford CT Google Scholar, 2013.